ACS APPLIED MATERIALS & INTERFACES

Research Article

www.acsami.org

Self-Assembled Molecular Platforms for Bacteria/Material Biointerface Studies: Importance to Control Functional Group Accessibility

Judith Böhmler, Arnaud Ponche, Karine Anselme, and Lydie Ploux*

Institut of Materials Science of Mulhouse (CNRS UMR7361), Mulhouse, France

Supporting Information

ABSTRACT: Highly controlled mixed molecular layers are crucial to study the role of material surface chemistry in biointerfaces, such as bacteria and subsequent biofilms interacting with biomaterials. Silanes with non-nucleophilic functional groups are promising to form self-assembled monolayers (SAMs) due to their low sensitivity to side-reactions. Nevertheless, the real control of surface chemistry, layer structure, and organization has not been determined. Here, we report a comprehensive synthesis and analysis of undecyltrichlorosilane- and 11-bromoundecyltrichlorosilane-based mixed SAMs on silicon substrates. The impact of the experimental conditions on the control of surface chemistry, layer structure, and organization was investigated by combining survey and high-resolution X-ray photoelectron spectroscopy analysis, wettability measurements, and ellipsometry. The most appropriate conditions were first determined for elaborating highly reproducible, but easily made, pure 11-bromoundecyltrichlorosilane SAMs. We have demonstrated that the control is maintained on more complex surfaces, i.e., surfaces revealing various chemical densities, which were obtained with different ratios of undecyltrichlorosilane and 11-bromoundecyltrichlorosilane. The control is also maintained after bromine to amine group conversion via S_N2 bromine-to-azide reactions. The appropriateness of such highly controlled amino- and methyl-group revealing platforms (NH_2−X%/CH_3) for biointerface studies was shown by the higher reproducibility of bacterial adhesion on NH_2−100%/CH_3 SAMs compared to bacterial adhesion on molecular layers of overall similar surface chemistry but less control at the molecular scale.

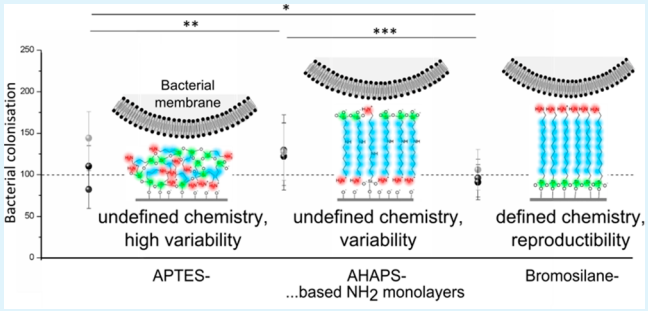

KEYWORDS: *biointerface, bacterial adhesion, surface chemistry, surface heterogeneity, model surfaces, SAMs, high-resolution XPS*

1. INTRODUCTION

Biointerfaces have become a crucial field of material science with applications as different as microfluidic systems, biosensors, and biomaterials. Certainly, understanding phenomena and mechanisms occurring at interfaces between materials and biological objects is the key to success for the development of new materials and coatings. Therefore, more and more investigations attempt to improve the fundamental knowledge in this area,[1−4] focusing on impacts of surface chemical,[5−8] topographical,[9−13] or mechanical properties.[14,15] In the specific frame of biomaterials-related infections, a crucial yet so far neglected topic concerns whether bacteria−material interfaces may be controlled by the material surface chemistry exhibited at the molecular scale. Chemical heterogeneity of the surface, accessibility, or orientation of (bio)molecules adsorbed or grafted at this interface are some of the parameters able to potentially affect the bacterial response to the surface. However, adequate material surfaces to specifically study this aspect are rare. They should be as ideal as possible to avoid side effects resulting from other surface characteristics (typically surface topography). They must be highly controlled and thoroughly described to know as exactly as possible the surface in contact with the microbial cell or biofilm under investigation.[4]

The best candidates for developing surfaces with a high control of extreme surface chemistry, layer structure, and molecular organization are probably self-assembled monolayers (SAMs).[16−18] Aside from providing a high-quality level of structure and architecture of the molecular layer,[19,20] they can in principle reveal a large diversity of functionalities by choosing the adequate molecular candidates.[19] They can also allow various ways of further grafting a large variety of molecules including biomolecules.[21] Besides, they can be stable enough to be used in long-term aqueous aging conditions or in *in vivo* mimicking experimental set-ups like bioreactors or flow cells.[7,22,23] If realized on silicon wafers, their high substrate smoothness is an additional advantage to achieve platforms for biointerface studies, avoiding any undesired effect of the surface micro- or nanotopographies. Chemically mixed monolayers can

Received: May 23, 2013
Accepted: October 9, 2013
Published: October 9, 2013

also be achieved on the basis of the same concept, allowing for specific studies about the roles of chemical heterogeneities and molecular accessibility in the adhesion of bacteria to surfaces.

Many studies about surface−bacteria interfaces conducted on molecular layers similar to SAMs have provided a number of relevant results.[7,22−26] Mainly, the molecular layer was expected to have a homogeneous, chemical composition. More rarely have chemically mixed molecular platforms based on SAMs been reported in this microbiological context. Wiencek and Fletcher proposed promising SAMs of mixed chemical composition with which they investigated bacterial behaviors in response to surface chemistry mainly described in terms of wettability.[27,28] Burton et al. developed mixed monolayers revealing gradients of chemical density, which were used for determining bacteria and mammalian cell adhesion variations in response to changes in carbon, oxygen, and nitrogen surface content.[29] Nevertheless, despite the undisputable interest of these mixed surfaces, the difference in length of the molecules used to create the molecular layer may have led to side effects due to topographical features at the molecular scale or chemical groups carried by the molecular main chains. In other words, as evoked by Wiencek and Fletcher, the biological response observed on such surfaces may be the result of several added or coupled effects.[28] To avoid roughness-related coupling effects, another approach of chemically mixed monolayers on silicon wafer should be used.

We propose to exploit an alternative way to create chemically mixed monolayers with silanes of identical length and a reduced risk of polymerization. Initiated by Heise et al. but never developed for biointerface studies, this approach exploits silanes with non-nucleophilic functional groups like bromine- and methyl-terminated trichlorosilanes.[30,31] Furthermore, *in situ* transformation (S_N2 reaction) allows the conversion of bromine groups into azide groups[32] to finally obtain amino mixed monolayers suitable for potential further grafting.[33,34] Promising platforms were obtained, providing good control of the densities of the chemical groups.[31] However, the composition and chemical purity of the organic layers were uncertain, preventing their use for studying the role of subtle surface chemical properties on biological objects. Moreover, experimental evidence of their structure and architecture has never been supplied. In the present study, mixed SAMs of high quality as well as a thorough description of their surface composition, structure, and organization are expected. This is achieved through adequate reaction conditions for platform synthesis and comprehensive analysis of their surface properties. We report evidence that this strategy supplies highly controlled and reproducible platforms for biointerface studies.

Trichlorosilanes with bromine and methyl groups are used as non-nucleophilic functional groups, and reaction conditions like concentration, solvent, temperature, reaction time, rinsing, and annealing are screened for elaborating fully covered (i.e., Br 100%) bromine surfaces. Subsequent changes in the surface properties are thoroughly analyzed through measurements of contact angle (sessile drop analysis), thickness in air and liquid environments (ellipsometry), elementary chemical composition (X-ray photoelectron spectroscopy survey spectra analysis), and chemical environments (X-ray photoelectron spectroscopy high-resolution spectra analysis). As we previously showed,[30] this association is expected to provide the necessary assurance of surface chemical composition, layer architecture, and structure, especially regarding potential defects such as impurities intercalated in the layer or undesired chemical side reactions. In a second part, mixed monolayers are synthesized using the reaction conditions that provide the most controlled layer characteristics. They are completely analyzed to confirm the control of surface chemical composition, layer structure, and organization, as well as their reproducibility. Conversion of bromine/methyl- to amino/methyl-revealing surfaces is also investigated. Finally, by comparing adhesion of bacteria on such fully amino-covered platforms (NH_2 100%) and on similarly amino-covered APTES and AHAPS SAMs, we evaluate whether these platforms may constitute an advantage to provide new and more relevant results in biointerface studies.

2. EXPERIMENTAL METHODS

2.1. Surface Substrate. Silicon wafer (100), purchased from MCR (Germany), one side polished, was used as a substrate for further chemical modification and cut into pieces of 1 cm × 1 cm. Substrate pieces were ultrasonically (frequency 45 kHz) cleaned for 10 min in $CHCl_3$ (Sigma-Aldrich) to remove organic contamination, followed by 30 min of cleaning in piranha solution (3:1 mixture of concentrated sulfuric acid to 30% hydrogen peroxide solution, both purchased by Sigma-Aldrich) at 50 °C. Samples were then rinsed with distilled Milli-Q water.

2.2. Chemical Modifications: NH_2-Terminated SAMs. In the following sections of the paper, the so-named "NH_2 100%" surfaces refer to surfaces exhibiting full coverage with amino groups in general, whatever the APTES-, AHAPS-, or Br-based mode of preparation.

3-Aminopropyltriethoxysilane (APTES)- and N-(6-aminohexyl)-aminopropyltrimethoxysilane (AHAPS)-Based SAMs. For the elaboration of amino-functionalized layers made of APTES, piranha-cleaned substrates were immersed in a 1 mM solution of 3-aminopropyltriethoxysilane (APTES, purchased from ABCR in Germany) in acetone (Sigma-Aldrich) overnight at room temperature in the dark. Samples were cleaned for 30 s in acetone under ultrasonic treatment (45 kHz) to remove the free silane fraction.

The same protocol was used for *N*-(6-aminohexyl)-aminopropyltrimethoxysilane (AHAPS, purchased from ABCR in Germany), respectively, in ethanol (Sigma-Aldrich). In the following sections of the paper, these two types of surfaces are named the "APTES-based NH_2 100 %" surface and "AHAPS-based NH_2 100 %" surface, respectively.

SAMs Based on Silane with a Non-Nucleophilic Functional Group: First Step (11-Bromoundecyltrichlorosilane-Based SAMs). Freshly cleaned substrates were immersed for 4 h in a solution of 70% *n*-heptane (n-C_7H_{16}, Carlo Erba) and 30% chloroform ($CHCl_3$, Sigma-Aldrich) at 6 °C containing various molar ratios of undecyltrichlorosilane and 11-bromo-undecyltrichlorosilane (ABCR, Germany) according to the desired bromine density, i.e., Br/CH_3 surface ratio.

Freshly prepared, piranha-activated wafers were immersed in a 1 mM solution of 11-bromo-undecyltrichlorosilane (ABCR, Germany). Several solvents (hexadecane, $CHCl_3$, heptane, toluene, and 30% $CHCl_3$ in heptane), temperatures (6, 20, and 45 °C), and immersion times (4 and 16 h) were tested (Table 1). Samples were then rinsed by immersion in $CHCl_3$ and hot water, before drying under nitrogen

Table 1. Reaction Conditions Used for Final Br 100% Surface Synthesis

parameters	reference reaction conditions[26]	modified reaction conditions
concentration of silane	1 mM	1 mM
solvent	hexadecane	70% *n*-heptane/30% $CHCl_3$
time	5 h	4 h
temperature	45 °C	6 °C
1. rinsing	$CHCl_3$/hot water	$CHCl_3$/hot water
annealing	none	1 h at 105 °C
2. rinsing	none	15 min sonication in $CHCl_3$

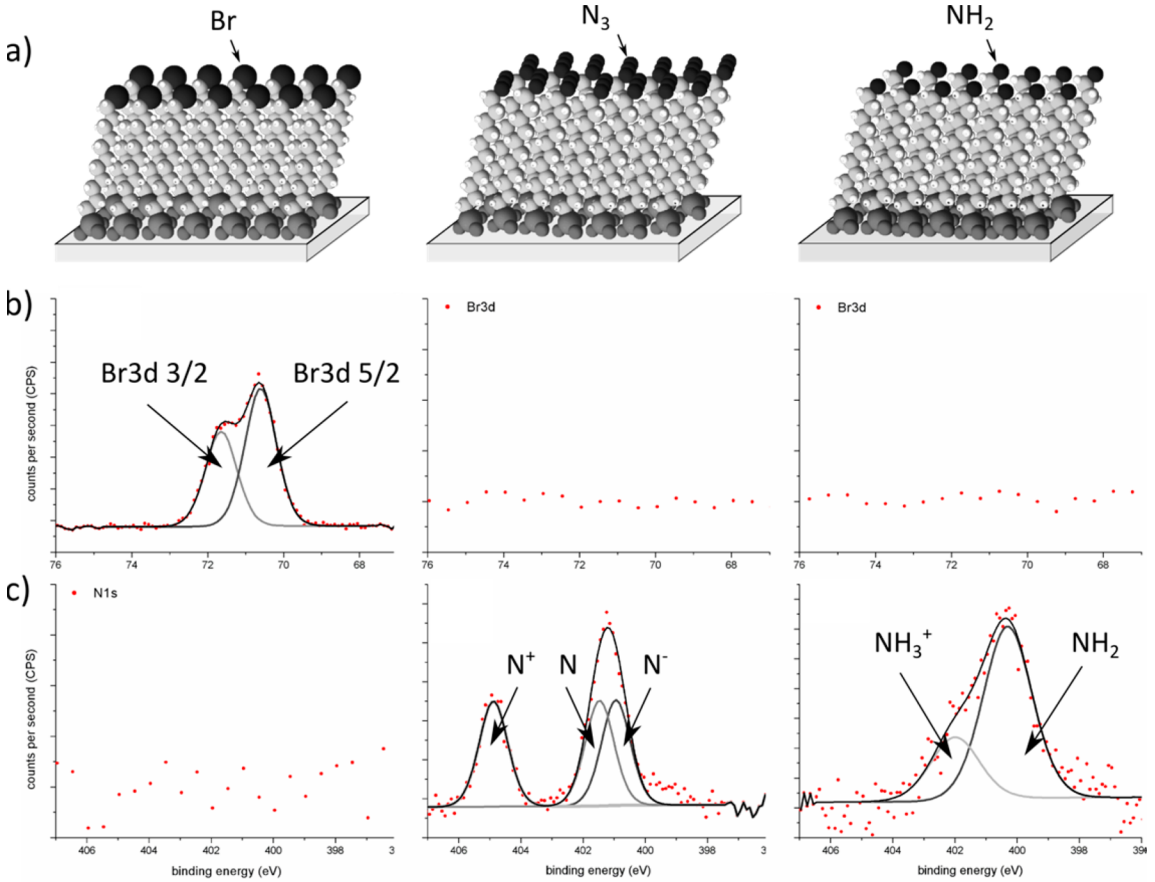

Figure 1. (a) Scheme of the conversion of bromine-revealing to amino-revealing surfaces: bromine groups are converted by a S_N2 reaction to azide groups that are subsequently converted to amino groups. (b) Br3d high-resolution XPS spectra associated with Br 100%, N_3 100%, and Br-based NH_2 100% surfaces, respectively (from left to right). (c) N1s high-resolution XPS spectra associated with Br 100%, N_3 100%, and Br-based NH_2 100% surfaces, respectively.

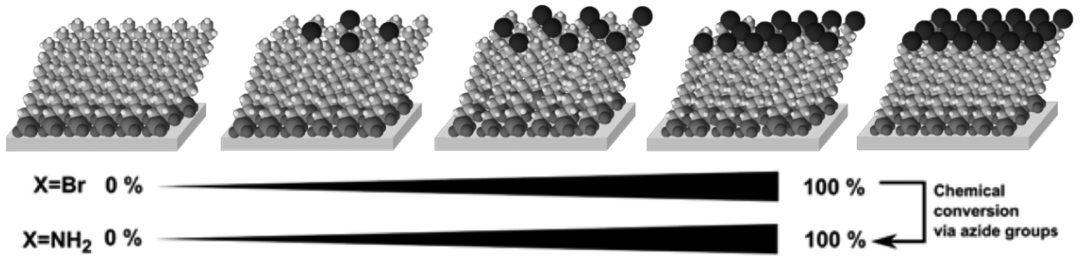

Figure 2. Principle of the mixed monolayers production. Five smooth surfaces with five different surface fractions (0, 25, 50, 75, and 100%) of Br groups in a CH_3 group environment are produced. Five surfaces with five different surface fractions (0, 25, 50, 75, and 100%) of NH_2 groups in a CH_3 group environment are obtained after chemical conversion of Br to NH_2 groups via S_N2 conversion and further amino reduction. Br/CH_3 and NH_2/CH_3 surfaces are smooth and highly controlled in terms of surface chemical composition and structure and organization of the silane layers.

stream. Improvement of stability potentially resulting for an additional annealing and ultrasonic treatment step was tested. For that purpose, functionalized samples were baked for 1 h at 105 °C, and subsequently ultrasonically rinsed for 15 min in $CHCl_3$ to remove residual silanes. The final surface is named the "Br 100%" surface in the following sections.

SAMs Based on Silane with a Non-Nucleophilic Functional Group: Second Step (Conversion of Bromine to Amino Termination). S_N2 nucleophilic substitution and subsequent reductive amination were performed on Br 100% surfaces to convert them into azide-terminated surfaces ("N_3 100%" surfaces) and finally into amine-functionalized surfaces ("Br-based NH_2 100%" surfaces)[30,33] (Figure 1a). To convert bromine to azide functional groups, bromine-functionalized samples were immersed in a 0.23 M solution of sodium azide (NaN_3, Fluka) in dimethylformamide (DMF, Sigma-Aldrich) under shaking for 6, 12, 24, or 72 h at room temperature for the study of S_N2 reaction kinetics, for 72 h for further processing, i.e., amination. Samples were then rinsed with Milli-Q water and acetone before drying under a nitrogen stream. Subsequently, azide-revealing samples were reduced overnight by immersion in a 0.2 M solution of lithium aluminum hydride ($LiAlH_4$, Sigma-Aldrich) in tetrahydrofuran (THF, Carlo Erba) before being immersed in THF over 12 h at room temperature. Lithium complexes on the surface were removed by hydrolysis for 1 h in a 10% solution of hydrochloric acid (HCl, 37%, Sigma-Aldrich). Samples were then rinsed with Milli-Q water and ethanol (C_2H_5OH, 99.9% absolute anhydrous, Carlo Erba) before drying under a nitrogen stream. Finally, the resulting NH_3^+ groups were converted into NH_2 groups by immersion in triethylamine (TEA, Sigma-Aldrich) for 24 h at room temperature. Samples were finally rinsed with Milli-Q water (pH between 5.0 and 5.8) and ethanol

before drying under a nitrogen stream. The final surfaces are called "Br-based NH_2 100%" surfaces in the following sections.

2.3. Chemical Modifications: Br/CH_3 and NH_2/CH_3 Mixed Self-Assembled Monolayers (MMLs). Freshly cleaned substrates were immersed for 4 h in a solution of 70% *n*-heptane (*n*-C_7H_{16}, Carlo Erba) and 30% chloroform ($CHCl_3$, Sigma-Aldrich) at 6 °C containing various molar ratios of undecyltrichlorosilane and 11-bromo-undecyltrichlorosilane (ABCR, Germany) according to the desired bromine density, i.e., Br/CH_3 surface ratio. Five bromine surface fractions were considered: 0, 25, 50, 75, and 100% (Figure 2). The final concentration of silane(s) in solution was constant and equal to 1 mM. Samples were rinsed with chloroform and shortly immersed in hot water. Subsequently, they were baked for 1 h at 105 °C before rinsing for 10 min in chloroform under ultrasonic treatment. In further sections, these final surfaces are named "Br *X*%" surfaces, according to the expected surface coverage in bromine. A Br 100% surface is expected to exhibit only Br groups at the extreme surface.

Br *X*% surfaces were further converted into so-called "NH_2 *X*%" surfaces by using the same procedure as described in paragraph 2.2.2 (Figure 1). As each molecule of silane contains 11 carbons for one nitrogen atom, the NH_2 *X*% surface is expected to reveal a NH_2 to CH_3 functional group ratio of *X*%.

2.4. Surface Characterization. Survey and high-resolution X-ray photoelectron spectroscopy (XPS), ellipsometry, atomic force microscopy (AFM), and contact angle measurements were used to determine the chemical composition, the structure, and the organization of the layers.

X-ray Photoelectron Spectroscopy (XPS). XPS analysis was used to determine the chemical composition of the surface layers. It was performed with a Gammadata Scienta spectrometer equipped with a monochromated Al Kα X-ray source (1486.6 eV) under ultrahigh vacuum (base pressure <10^{-9} mbar) and a takeoff angle of 90°. Survey and high-resolution spectra were recorded at pass energies of 500 and 100 eV, respectively. For high-resolution experiments, the overall energetic resolution is estimated to be 0.45 eV. All spectra were analyzed and peak-fitted using CasaXPS 2.3.12 software (Casa Software Ltd., Teignmouth, U.K., www.casaxps.com). All components were referenced according to the CHx component at 285.0 eV, and the full width at half-maximum (fwhm) was constrained to be constant for all components in the same high-resolution spectrum. The relative binding energy of all components was fixed and maintained constant for all peak-fitting procedures. The sensitivity of the spectrometer allowed the separation of the CHx (285.0 eV) component from the C−Br (286.0 eV) and of the $Br3d_{5/2}$ (70.6 eV) component from the $Br3d_{3/2}$ (71.6 eV), the two components due to spin orbit coupling of photoelectrons emitted from Br3d orbitals.

X-ray Photoelectron Spectroscopy (XPS): Surface Fraction Calculation. For Br/CH_3 MML, the experimental Br surface fraction was evaluated by two approaches leading to eqs 1 and 2. Equation 2 precisely evaluates the ratio of Br-terminated to CH_3-terminated silanes present on the surface, while eq 1 is sensitive to the presence in the organic layer of all C-containing molecules including solvent and other contaminants. Both equations originate in the composition of the Br-terminated and CH_3-terminated silanes (for eq 1: 1 bromine atom and 11 carbon atoms per Br-terminated molecule, while no bromine atom and 11 carbon atoms per CH_3-terminated molecule; for eq 2: 1 bromine group and 10 carbons under the CHx form per Br-terminated molecule, while no bromine group and 11 CHx groups per CH_3-terminated molecule). For eq 2, the CHx component was preferred to C−Br, since its peak displayed higher intensity and less sensitivity to peak fitting conditions. In addition, the uses of the $Br3d_{3/2}$ and $Br3d_{5/2}$ components are equivalent. The $Br3d_{5/2}$ component was arbitrarily used for calculations in eq 2. The experimental Br/SiOx atomic composition ratio was evaluated by eq 3, providing an indication of substrate coverage in comparison to the substrate reference, i.e., ungrafted silicon wafer. For this, the XPS signal associated with the SiOx component in the Si2p component (Supporting Information, Figure 1) was used. For NH_2/CH_3 MML, the experimental NH_2 surface fraction was only evaluated by eq 2. The total area of the N1s component peak was used for calculations, including both NH_2 and NH_3^+ groups. For all peak quantifications, area values were corrected by using Scofield sensitivity factors (Br3d, 2.84; $Br3d_{5/2}$, 1.68; C1s, 1.00; CHx, 1.00; N1s, 1.80; SiOx, 0.82). Ratios of corrected areas were determined for Br3d/C1s, Br3d/$Si2p_{SiOx}$, $Br3d_{5/2}$/CHx, and N1s/CHx components on high-resolution spectra.

$$X_{C1s}\ (\%) = \frac{A(\mathrm{Br3d})}{A(\mathrm{C1s})} \times 11 \times 100 \tag{1}$$

where X_{C1s} (%) is the molar surface fraction of bromine groups, A(Br3d) is the corrected area of Br3d, and A(C1s) is the corrected area of the C1s component (total carbon content determined on the survey spectrum).

$$X_{CHx}\ (\%) = \frac{\frac{A\left(\mathrm{N1s\ or\ Br3d\frac{5}{2}}\right)}{A(\mathrm{CHx})}}{1 + \frac{A\left(\mathrm{N1s\ or\ Br3d\frac{5}{2}}\right)}{A(\mathrm{CHx})}} \times 11 \times 100 \tag{2}$$

where X_{CHx} (%) is the molar surface fraction of bromine or amine groups, A(N1s) is the corrected area of N1s, A(Br3d(5/2)) is the corrected area of $Br3d_{5/2}$, and A(CHx) is the corrected area of the CHx component in the high-resolution C1s spectrum.

$$\frac{\mathrm{Br}}{\mathrm{SiOx}} = \frac{A(\mathrm{Br3d})}{A(\mathrm{Si2p_{SiOx}})} \tag{3}$$

where Br/SiOx is the molar surface fraction of Br compared to the substrate in its oxidized form, A(Br3d) is the corrected area of Br3d, and $A(Si2p_{SiOx})$ is the corrected area of the SiOx component determined on the high-resolution Si2p spectrum.

X-ray Photoelectron Spectroscopy (XPS): Kinetics of the S_N2 Reaction. Conversion from bromine to azide groups was investigated on Br 100% surfaces after 6, 12, 24, and 72 h of S_N2 reaction. The surface fraction of Br was determined on the basis of the $Br3d_{5/2}$ and CHx components, by using eq 2 as described above. The surface fraction of N_3 was calculated with eq 4, knowing that the typical signal of azide groups measured with high-resolution XPS displays three nitrogen components (positively —N^+—, neutral —N—, and negatively —N^-— charged nitrogen atoms) associated with two azide mesomers (R—N^-—N^+≡N ↔ R—N=N^+=N^-) (Supporting Information, Figure 2). After peak fitting, the areas of the three resulting peaks were corrected by using Scofield sensitivity factors as specified above.

$$X_{CHx}\ (\%) = \frac{A(\mathrm{N^+}) + A(\mathrm{N}) + A(\mathrm{N^-})}{A(\mathrm{CHx})} \times \frac{1}{3} \times 100 \tag{4}$$

where X_{CHx} (%) is the molar surface fraction of azide groups and $A(N^+)$, A(N), and $A(N^-)$ are the corrected areas of N^+, N, and N^- components in the N1s spectrum.

Contact Angle Measurements. Water contact angles were measured for assessing wettability and the hydrophilic/hydrophobic character of the surface layers. Static, advancing, and receding contact angles were measured as described elsewhere,[35] at room temperature with a contact angle goniometer (Krüss) coupled to a camera and an image analyzer. The static contact angle (θ_s) was determined after a delay of 1 min to ensure the equilibration of the droplet (2 μL of Milli-Q water, pH 5.8). Reported values are an average of measurements performed at three different regions on four different samples. Hysteresis, defined as the difference between advancing (θ_a) and receding (θ_r) contact angles, was used as a quantitative indication of surface homogeneity. In general, small and large values are, respectively, a sign of homogeneous and heterogeneous surface properties.[36]

Ellipsometry. Ellipsometry was used to determine the thickness of the layers as described elsewhere.[35] Briefly, measurements were done at 532 nm (HeNe laser) and an incident angle of 70° with an ellipsometer equipped with a phase modulation multiskop from Physik Instrument (modelM-O33K001). The thickness of the chemical, grafted layers was evaluated at room temperature both in air (named

"thickness in air") and in Milli-Q water (named "thickness in liquid"). Δ and ψ values were measured on three different regions of each sample. The thickness of the oxide layer was determined on ungrafted silicon wafers cleaned as described in section 2.1. Models were composed of two (pure silicon and oxide layer) or three layers (pure silicon, oxide layer, and organic layer) for ungrafted and grafted silicon wafers, respectively. Refractive indices were those reported previously.[35]

Atomic Force Microscopy (AFM). AFM was used to determine surface morphology and surface roughness. A NanoScopeIII/Dimension 3000 (Digital Instrument) equipped with a Si cantilever (k = 42 N/m, Pointprobe, Nano World) was used in tapping mode under ambient air, with a scan rate of 1 Hz and image size of 2 μm^2. AFM micrographs were analyzed with the NanoScope 6.13R1 software (Digital instrument) for providing a mean roughness values (Ra, arithmetic average of the absolute height values). With height and phase contrast micrographs being similar, only height images are considered for discussion.

2.5. Biointerface Experiment. Bacterial adhesion intensity and repeatability on the three differently synthesized NH_2 100% surfaces of theoretically similar surface chemical composition (APTES-, AHAPS-, and Br-based NH_2 100%) were compared.

Bacterial Strain and Culture. Bacterial experiments were conducted with *Escherichia coli* (*E. coli*) MG1655.[37] Frozen bacteria (−80 °C) were cultured overnight on Luria Bertani (LB purchased from Sigma-Aldrich) agar plates at 30 °C. A first preculture was then prepared with one colony in LB and incubated overnight at 30 °C. A second preculture (10% of the first preculture) was prepared in M63G selective medium[37] and incubated overnight at 30 °C. A third preculture (10% in M63G of the second preculture) was incubated for 4 h before centrifugation for harvesting bacteria. Bacteria were then resuspended in M63G to reach an absorbance of 0.01 at 600 nm.

Bacterial Adhesion Test. NH_2 100% surfaces (APTES-, AHAPS-, and Br-based NH_2 100%) were inoculated with the bacterial suspension at 0.01 of 600 nm absorbance. Hence, bacteria were cultured for 2 h on the samples before nonadherent bacteria were removed by five subsequent gentle rinsing steps with a sterile NaCl (9 g/L) solution. Visualization of bacteria was performed by fluorescent confocal microscopy (Zeiss Upright LSM700) after bacteria staining with Syto9 (Molecular Probes, 1 μL/mL of a 5 mM Syto9 stock solution). Bacteria were observed directly in the last rinsing solution using a 9 mm long focal objective (Zeiss LD Epiplan Neofluar 50×). The experiment was repeated three times. Two samples of each type were used for one experiment. Ten zones per sample were microscopically imaged. On each micrograph, the number of adherent bacteria was determined through image analysis by using ImageJ V1.44d software with LSMtoolbox V4.0g plugins.[38] The average and standard deviation of adherent bacteria numbers were calculated for each sample and each experiment. Significant two-by-two differences between numbers of adherent bacteria on APTES-, AHAPS-, and Br-based NH_2 100% surfaces were evaluated by Student's t-tests.

3. RESULTS AND DISCUSSION

3.1. Control of Monolayer Chemical Composition, Layer Structure, and Organization. To synthesize platforms for biointerface studies, functionalization of silicon wafers with organosilane-based SAMs should allow control of surface chemistry at the molecular scale without adding any roughness side-property.[20] SAMs have an organization typical of two-dimensional polysiloxane networks and have long-term stability, both characteristics originating from the van der Waals interactions that occur along the main chain of the organosilanes.[19,20] To achieve this, organosilanes have to possess specificities already well described in the literature. Carbon main chains must be composed of more than 11 carbon atoms to avoid formation of multilayers.[39] Functional groups have to be small enough to avoid steric hindrance, then allowing closely packed assembling,[32,40] and must be unable to compete with the head groups for interacting with the surface.[32,35,41] Additionally, reaction conditions during SAM synthesis are crucial: temperature, reaction time, solvent(s), and additional annealing in particular have been reported for their influence.

Mixed monolayers with highly controlled chemical group densities, layer structure, and organization can be envisaged on this basis. The most successful mixed monolayers that were based on SAMs and exhibited roughness-free surfaces were reported in the literature by Heise et al.[30] They were obtained with undecyltrichlorosilane and 11-bromoundecyltrichlorosilane. The relationship between the composition of silane on the surface and the content of silane in the silanization solution was quasi-linear, revealing a good control of the surface chemical composition. Moreover, thickness measurements were consistent with a monolayer structure. However, the surface fraction in the bromine group was much lower than expected for pure and highly packed SAMs (60% rather than 100% for 100% bromine-revealing monolayer). Intercalation in the silane monolayer of undesirable organic molecules, such as solvent, and/or underestimation of the surface fraction value due to monolayer degradation during the XPS analysis with a non-monochromatic source may have resulted in this low value. The chemical composition was, therefore, uncertain. In addition, spot-like aggregates were reported, suggesting defaults in the coating structure. The absence of survey spectra and Br to substrate (Si) atomic composition ratios that are lower than expected also prevented the confirmation of close-compactness of the grafted silanes.

We developed a protocol to provide Br 100%, Br 75%, Br 50%, Br 25%, and Br 0% mixed monolayers (Br backfilled with CH_3) of high quality in terms of chemical composition, structure, and organization. Efforts were first turned to Br 100% before applying identical synthesis conditions to create surfaces with other Br/CH_3 ratios. Reaction conditions consistent with the standard opportunities offered by biointerface laboratory environments (room temperature or low positive temperature as reached by a refrigerator, for example) were voluntarily preferred. Particular attention was also given to the comprehensive description of the monolayer. Surface and layer characteristics such as chemical composition, structure, and organization were determined on the main basis of high-resolution XPS analysis, with systematic comparison to experimental results provided by ellipsometry, contact angle measurements, and AFM.

Reaction conditions used in the work published by Heise et al.[30] and having provided the most successful mixed monolayers were considered as reference conditions (see Table 1). Characteristics of the layers obtained in the present work with this approach (Table 2 and Supporting Information, Table 1) were significantly different than those reported by Heise et al.[30] In particular, the Br surface fraction was much higher (~100% both for Br_{C1s} and Br_{CHx}) than estimated from the published results (Br_{C1s} ~ 60%) and no spot-like aggregates were observed on the surfaces. Nevertheless, by reproduction of the reference protocol in the laboratory, contact angle hysteresis, which came as supplementary information compared to published work, was of high value, suggesting the presence of topographical defects at the extreme surface. Moreover, thickness values measured in air or in liquid were 10 times higher than expected (1.4 nm), demonstrating that the silane layer did not reveal the typical monolayer structure expected for SAMs.

Table 2. Characteristics of Br 100% Layers Obtained in the Two Different Sets of Reaction Conditions, as Described in Table 1[a]

	reference reaction conditions[26]	modified reaction conditions
Br_{CHx} (%)	107 ± 2	105 ± 5
Br_{C1s} (%)	95 ± 3	91 ± 5
Br/SiOx	0.42 ± 0.05	0.15 ± 0.02
θ_s (deg)	88 ± 2	86 ± 1
θ_a (deg)	102 ± 2	94 ± 1
θ_r (deg)	70 ± 2	72 ± 3
ΔH (deg)	32	22
$thickness_{air}$ (nm)	11.7 ± 3.6	1.5 ± 0.2
$thickness_{liquid}$ (nm)	10.5 ± 2.8	1.6 ± 0.2

[a]Measurements have been done at least three times.

Diverse protocol modifications in terms of annealing and ultrasonic post-treatments, solvents, temperatures, and reaction times were considered, allowing the achievement of characteristics presented in Table 2. Thickness of the layer, measured in water, was in very good agreement with the theoretical value (1.6 ± 0.2 nm compared to 1.4 nm), and the Br/SiOx ratio also reached an experimental value close to the estimated one (0.11; see Supporting Information, Figure 3, for calculation), which indicated that monolayers were achieved. Importantly, a high Br surface fraction (Br_{CHx} of 105 ± 5%) and experimental values of contact angle (θ_e of 86 ± 1°) in very good agreement with published values (80−89° according to Aswal et al.[21]) were maintained compared to reference reaction conditions, assuring that layer structure improvement was not accompanied by degradation of the dense packing of silanes. Eventually, the quality of the silane layer was significantly improved with the modified reaction providing highly structured and packed Br 100% SAMs.

Modifications in the reaction conditions and subsequent changes in layer characteristics, which have led to the above Br 100% SAMs, are illustrated in Figure 3. Annealing and subsequent ultrasonic post-treatments were aimed at improving the stability of the silane layers for their use in aqueous media during long-term biological experiments. Removal of the water layer present at the silane−substrate interface was expected to allow the chemisorption of silanes to substrate instead of physical adsorption, while silane molecules present in the molecular layer, yet not bound to the substrate, should be removed by thorough rinsing under ultrasonic conditions.[42,43] Accordingly, the thickness of the silane layer slightly decreased (Figure 3a) without reduction of the Br_{CHx} surface fraction (Figure 3b and c). An increase in the Br/SiOx ratio measured after annealing and ultrasonic treatment indicates that the stability of the silane layer under high-vacuum XPS conditions was improved (Figure 3d). The solvent used for silane solutions was chosen to improve silane solubility for a better subsequent organization of silanes grafted on the substrate. Among five tested solvents (hexadecane, chloroform, heptane, toluene, chloroform/heptane mixture), the chloroform/heptane mixture allowed a reduction of layer thickness (1.2 ± 0.0 nm measured in air) tending to theoretical thickness of a monolayer (1.4 nm) (Figure 3a) without degradation of the Br surface fraction (Br_{CHx} ~ 100%) (Figure 3b and c). The layer was then shown to have a monolayer structure free from organic contaminants structure. Nevertheless, a slight difference between experimental and theoretical (1.4 nm) thickness values indicated

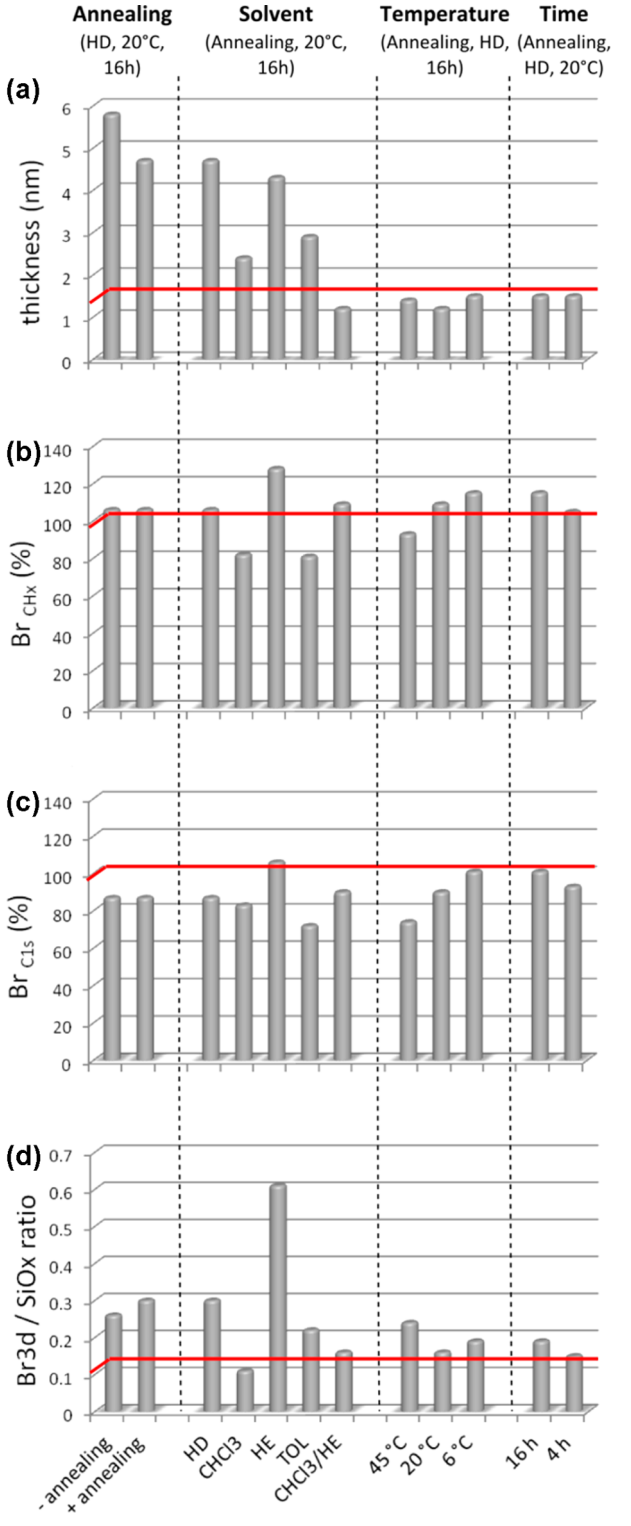

Figure 3. Characteristics of Br 100% layers obtained in different reaction conditions in terms of post-treatments, including an annealing step and further rinsing under sonication, solvent (hexadecane, HD; heptane, HE; toluene, Tol; chloroforme, $CHCl_3$; heptane/chloroforme, $CHCl_3$/HE), temperature, and reaction time. The thickness of the organic layers (a) was determined by ellipsometry, Br surface fractions were calculated on the basis of the CHx component (Br_{CHx}) (b) or on the basis of the C1s component (Br_{C1s}) (c), and the surface fractions of SiOx substrate covered by Br (Br/SiOx) (d) were determined by high-resolution XPS. They are reported for the different reaction conditions. Red lines indicate the expected, theoretical values.

dx.doi.org/10.1021/am401976g | ACS Appl. Mater. Interfaces 2013, 5, 10478−10488

insufficient dense packing of the assembled silanes. Improvement of the compactness was obtained by decreasing the reaction temperature to 6 °C according to the studies of Brozska et al. on the optimization of monolayer formation with 11-carbon-chain silanes.[39,40,43] Time reaction modification was also investigated in order to increase layer compactness. Slight changes in Br content of the layer were observed as demonstrated by Br_{CHx} and Br_{C1s} surface fractions and the Br/SiOx ratio (Figure 3b, c, and d, respectively), without modification of layer thickness (Figure 3a), suggesting an increase of layer compactness with increasing reaction time. For practical reasons, including the necessity to rapidly perform Br to NH_2 conversion steps after making Br *X*% MMLs, a reaction time of 4 h was preferred to 16 h, without degradation of the layer quality.

3.2. Mixed Monolayers. Mixed monolayers of different Br surface fractions in CH_3 were fabricated by using the reaction conditions developed for the Br 100% monolayer. The possibility to control Br surface fractions while reaching a high level of monolayer structure and organization as well as dense packing of silane was tested through a similar characterization approach as above. Five different surface fractions of Br in CH_3 were considered: 0, 25, 50, 75, and 100%.

As shown in Figure 4a, the Br solution content versus the Br coverage relationship was quasi-linear, which indicates that the chemical surface properties in terms of Br to CH_3 surface fraction can be controlled by proportionally adapting the content of bromine in the initial solution. No preferential adsorption of Br- versus CH_3-terminated silane was observed in contrast to the results reported by Heise et al.[30] Whether reaction conditions may be involved in the existence or the lack of preferential adsorption in silane mixtures has been suggested by other authors, but the question has not been elucidated yet.[43] A significantly higher Br surface fraction was achieved compared to that reported in the literature, as already noted above for Br 100%, indicating excellent purity and close packing of the grafted layer as well as nondestructive XPS analysis. Well control of surface chemical content and purity of the grafted layer were confirmed by the hydrophobic character of the surface (Figure 4b) that is in the same range as reported in the literature (85−110°) and decreases with Br content increase. This especially proves the absence of interactions between water drops used for contact angle measurement and the underlying silicon substrate, demonstrating that silanes are highly densely packed in the layer. Thickness measurements of the different Br *X*% layers, all in good agreement with the theoretical value, showed in addition that the silane layer displayed a monolayer structure whatever the Br to CH_3 surface fraction (Figure 4b). Finally, mixed Br/CH_3 monolayers were obtained with a similar, high level of control of chemical composition, layer structure, and organization as the Br 100% monolayer.

3.3. Conversion of Bromine Termination to Amino Groups. Conversion of Br/CH_3 to NH_2/CH_3 mixed monolayers was performed via S_N2 bromine-to-azide conversion, as depicted in Figure 1a. The efficiency of conversion as well as maintenance of control of the monolayer properties over the Br to NH_2 conversion were investigated on the five Br mixed monolayers of different Br surface fractions, 0, 25, 50, 75, and 100%. The efficiency of the conversion steps was determined by using high-resolution XPS. The kinetics of the conversion reaction was investigated on the Br 100%

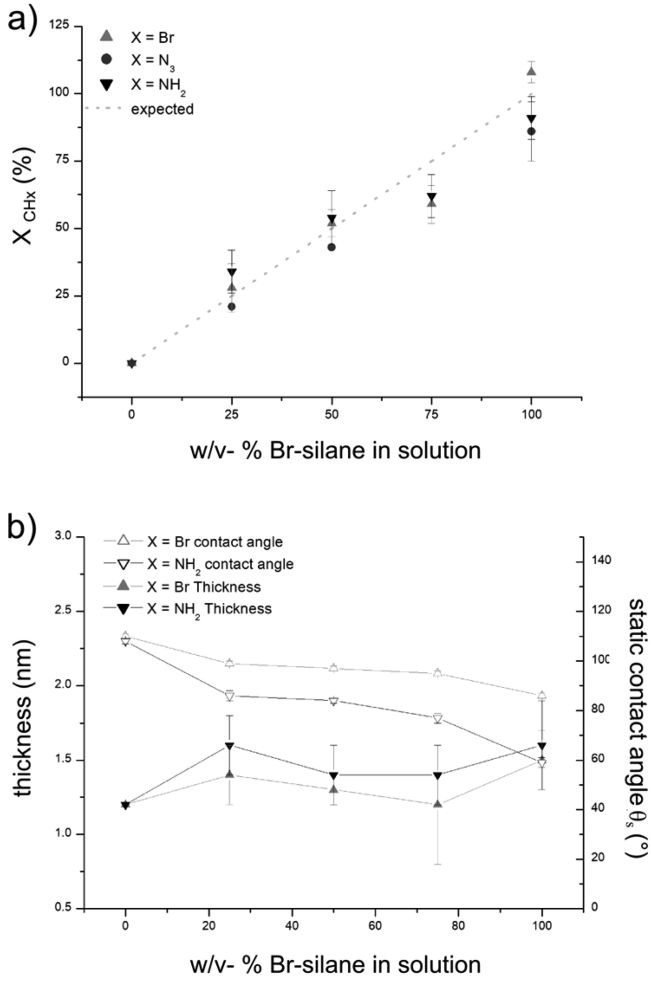

Figure 4. Experimental properties of five surfaces revealing different theoretical Br/CH_3, N_3/CH_3, and NH_2/CH_3 surface fractions (0, 25, 50, 75, and 100%). Five different concentrations of Br−silane solution were used to fabricate the five types of Br/CH_3 surfaces. N_3/CH_3 surfaces were obtained from Br/CH_3 surfaces after chemical conversions of Br to N_3 groups. NH_2/CH_3 surfaces were obtained from N_3/CH_3 surfaces after chemical conversions of N_3 to NH_2 groups. (a) Experimental surface fractions in Br, N_3, and NH_2 determined by high-resolution XPS and referred to CHx components (X_{CHx} with *X* = Br, N_3, or NH_2). (b) Static contact angles measured by the sessile drop method and thickness of the silane layers measured by ellipsometry.

monolayer. X_{CHx} for *X* = Br and *X* = N_3 were measured at various times of reaction between the Br monolayer and NaN_3 reactive agent. As shown in Figure 5, total conversion was achieved after 72 h of reaction, with high-resolution spectra showing the total disappearance of Br components and the detection of a N_3-typical spectrum (Figure 1b and c). The S_N2 kinetics are known to be fast under liquid conditions with leaving groups like bromine and strong nucleophiles like azide.[44] Nevertheless, the S_N2 reaction is also very sensitive to alkyl chain length and crowding effects around the leaving group. Consequently, S_N2 kinetics occurring on a surface are significantly slowed down compared to in liquid due to a limited accessibility of the reagents, as already stated by Fryxell et al.[32] This may be enhanced by the high packing of silanes on the surface, as suggested by the results shown above. The kinetics and total conversion after 72 h of reaction were confirmed for all five Br surface fractions (data not shown).

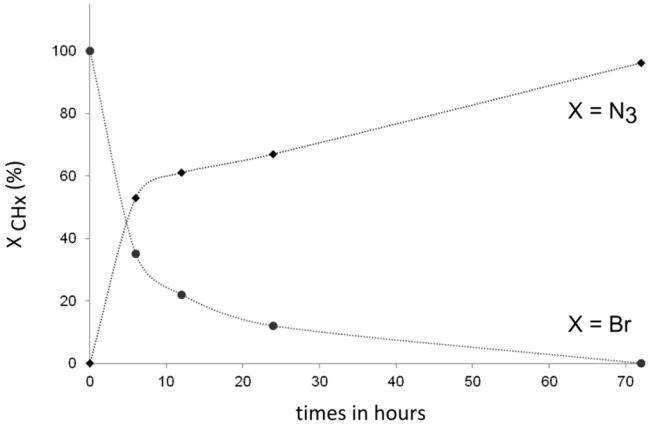

Figure 5. Kinetics of Br to N_3 conversion determined by high-resolution XPS. Surface fractions (X_{CHx}) of Br and N_3 were measured at 6, 12, 24, and 72 h reaction times of Br 100% surface with NaN_3.

Subsequent reduction of N_3 to NH_2 was also demonstrated to be complete for all N_3 *X*% layers, which is typically displayed by the complete conversion of N^+, N, and N^- to NH_3^+ and NH_2 components in high-resolution XPS spectra (Figure 1c). In addition to NH_2 groups, NH_3^+ functional groups (20 at. %) were detected, which may result from incomplete reduction of NH_3^+ groups during the postconversion treatment with triethylamine. In this hypothesis, counterions are then expected to be detected by XPS analysis. However, no signal corresponding to the most common counterions (especially Cl^-, HCO_3^-, and AlH_4^-) was detected on the survey spectra (Supporting Information, Figure 4). The second hypothesis is the sample charging under X-ray irradiation, i.e., during XPS analysis, by ejection of photoelectrons from the material. However, this phenomenon should affect all functionalities, which could not be stated in the present study. Consequently, the origin of the detected NH_3^+ groups has not been completely elucidated so far.

Analysis of the high-resolution XPS spectra also revealed that the linear relationship between the Br surface fraction and Br content of the initial solution was conserved after the first (from Br to N_3) and the second (from N_3 to NH_2) conversion steps (Figure 4). Nevertheless, the surface fraction in azide groups was systematically measured at lower values than expected through previous bromine. This is attributed to the chemical degradation of azide groups occurring through contact with air after preparation and potentially enhanced during XPS analysis.[45,46] Thermal and photochemical degradation may also be involved, even if thermodegradation is unlikely to occur, since samples are kept at room yet controlled temperature until analysis. Nevertheless, this did not impact the preparation of the amine surfaces, as shown by the very good agreement between the amine and bromine contents of the initial Br monolayers. Conversion led to NH_2/CH_3 mixed monolayers that displayed the expected chemical properties as further attested by the contact angle measurements (Figure 4b). Furthermore, as already discussed in the above paragraph, the good accordance between observed and expected contact angle values[21] certifies compactness of silanes in the monolayers and a high level of organization of the silanes, while thickness values, not modified by the chemical process, signify the monolayer structure. The monolayer structure was shown not to reveal domains of silane species, rather an intimate mixture at the molecular scale of both silane species. This is demonstrated by the relationship between $(1 + \cos\theta)^2$ and NH_2 surface content, where θ is reducing or advancing contact angle (Figure 6), according to Israelachvili et al.,[47] who

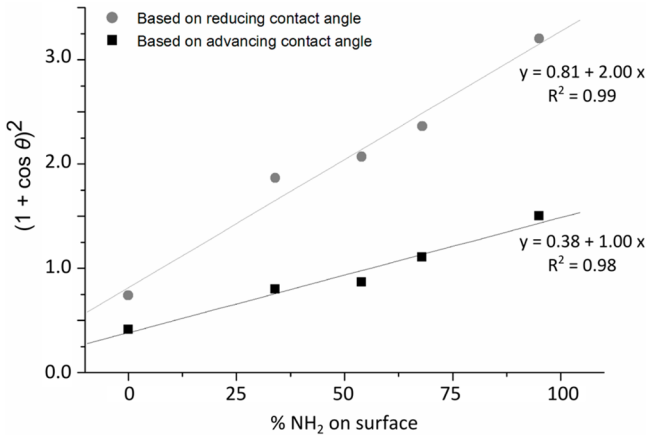

Figure 6. Relationship between $(1 + \cos\theta)^2$ and NH_2 content for NH_2 in CH_3 mixed monolayers of five different NH_2 surface fractions (0, 25, 50, 75, and 100%). According to Israelachvili et al.,[39] a linear relationship indicates chemical heterogeneity of the surface at the molecular or atomic scale, implying an absence of chemical domains on the surfaces.

associated the linear relationship to surface chemical heterogeneity at a molecular or atomic scale. Absence of domains in layers was confirmed by AFM images (Supporting Information, Figure 5). As displayed in Figure 7b for the Br-based NH_2 100% surface, real structure and organization of the mixed monolayer are, thus, estimated to be very close to the expected, ideal ones (Figure 7a). Finally, good reproducibility was maintained throughout the conversion from Br to NH_2 functional groups, shown by the low standard deviations of measurements of surface fraction, contact angle, and thickness values. The reproducibility of the monolayers is of high importance for their use in biointerface studies, due to the large quantities of ideally identical samples needed for such a purpose.

3.4. Relevance of the Br-Based NH_2/CH_3 Platforms for Biointerface Studies. Chemically homogeneous or mixed SAMs have already frequently been used for analyzing the influence of surface chemistry on bacterial adhesion and biofilm development. Three typical examples are the works reported by Katsikogianni et al.,[22,48] Ploux et al.,[7] and Wiencek et al.[27,28] Katsikogianni et al. used CH_3, NH_2, and OH terminated surfaces on glass substrates to investigate the adhesion of *S. epidermidis* on different surface chemistries after 2 h of culture under various hydrodynamic shear rates. They reported that the number of adherent bacteria decreased following the rank CH_3 > NH_2 > OH (pure glass slide). Ploux et al. used homogeneous NH_2 and CH_3 terminated layers on silicon wafers for studying the adhesion and proliferation of *E. coli* under static conditions in a time range from 4 h to 2 weeks. They reported similar colonization of NH_2 and CH_3 surfaces at 2 h but significantly different kinetics of biofilm formation as well as biofilm structure on NH_2 and CH_3 surfaces. By using mixed OH/CH_3 layers on gold substrates under hydrodynamic conditions, Wiencek et al. reported that the balance between bacterial attachment and detachment also leads to more bacterial attachment on CH_3 surfaces than on OH surfaces for *Pseudomonas sp.* In addition, the relationship between bacterial

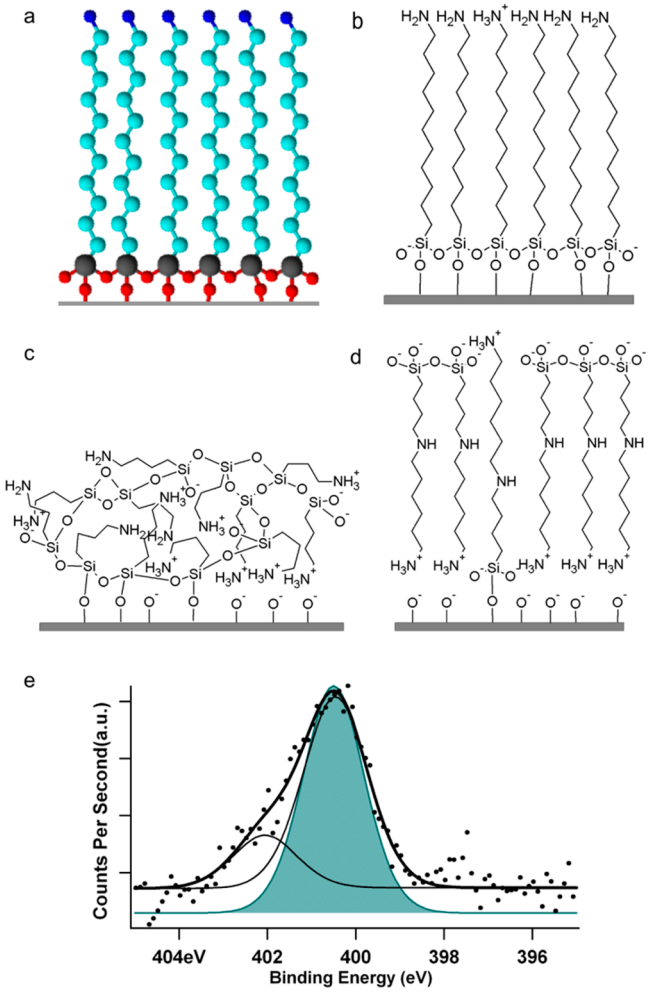

Figure 7. Representation of the "ideal" layer structure and molecular organization of Br-based NH_2 100% terminated surfaces (a). Representations of the "real" layer structure and molecular organization of NH_2 100% terminated surfaces based on Br–organosilane (b), APTES (c), and AHAPS (d). (e) XPS N1s high-resolution spectra expected for the ideal case (full curve) and for the real case (i.e., experimental results) (line curve) of Br–organosilane-based NH_2 100% terminated surfaces.

colonization and OH/CH_3 surface fraction was linear.[27,28] These examples illustrate that the results reported in different publications may appear as contradictory and are difficult to compare. Aside from differences in experimental approach, a comparison suffers from the absence of a comprehensive surface analysis, leading one to wonder whether possible structural and organizational failures may have altered the biological responses. Ligand posture for example was proposed by Fryxell et al. as a probable important factor of influence for biological interactions with surfaces.[49] Hence, sensitive effects potentially induced by subtle characteristics of surface chemistry to bacteria/surface interface, such as those related to functional group accessibility and chemical heterogeneity, may be screened by effects caused by unwished but stronger surface characteristics. The assurance that surface chemistry, structure, and organization of the Br-based NH_2/CH_3 mixed monolayers are highly controlled should, therefore, offer the opportunity to investigate subtle effects of surface chemistry, thus leading to new results in the bacteria/material interface field.

The relevance of highly controlled surfaces, such as Br-based NH_2/CH_3 mixed monolayers, for studying phenomena at material/bacteria interfaces was tested by comparing bacterial colonization and its variability on Br-based NH_2 100% surfaces and two other NH_2 100% terminated surfaces (APTES- and AHAPS-based NH_2 100% surfaces). APTES-based and, to a lesser extent, AHAPS-based NH_2 100% surfaces are frequently used in biointerface studies as typical amino surfaces. Nevertheless, both surface types are known to reveal defects in layer structure and/or silane organization in contrast to Br-based NH_2 100% surfaces (Figure 7b, c, and d).[35,41] Whether structural, organizational, and subsequent chemical composition defects can significantly impact experimental values, indicative of bacterial behavior, was thus tested here.

Average values of adherent bacterial numbers were measured for three independent experiments on APTES-, AHAPS-, and Br-based NH_2 100% surfaces (Figure 8). A two-by-two

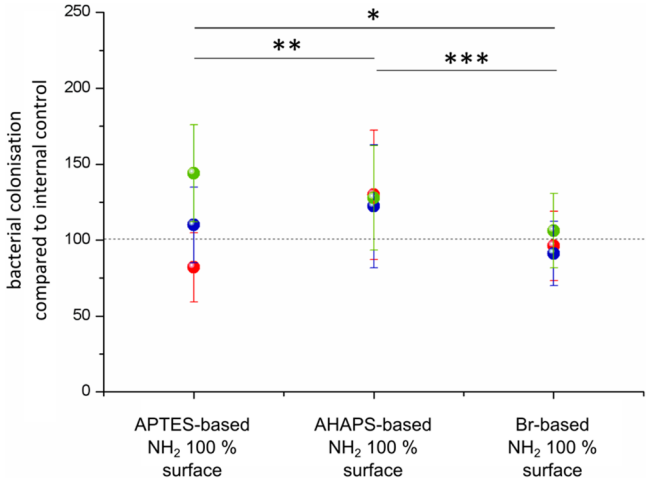

Figure 8. Amount of *E. coli* K12 (MG1655[32]) bacteria adhered on three different types of NH_2 100% surfaces (APTES-, AHAPS-, and Br-based NH_2 100% surfaces) compared to the internal control (i.e., cleaned, ungrafted silicon wafers; colonization of $(6.1 \pm 0.5) \times 10^5$ bacteria/cm^2). Averages calculated for three independent experiments are depicted (three different symbols) for each surface type. Each average value results from 20 measurements (adhered bacteria amount measured on 10 micrographs taken on two similar samples). *, **, and *** symbols correspond to significant differences between bacteria number averages with $p > 95.0\%$, $p > 99.0\%$, and $p > 99.9\%$, respectively.

comparison shows that adhered bacterial numbers were significantly different on the three NH_2 100% surface types (114 ± 35, 132 ± 32, and $102 \pm 14\%$, respectively, referred to internal control colonized by 6.1 ± 0.5 bacteria/cm^2). Remarkably, experimental deviations of adherent bacterial numbers determined for each type of NH_2 100% surface throughout the experiment replicas also highly differed between surface types. Bacterial number measurements on APTES- and AHAPS-based NH_2 100% surfaces, thus, varied by 35 and 32%, respectively, while variation was less than 14% on Br-based NH_2 100% surfaces. Differences in bacterial colonization could be directly attributed neither to variations of physical-chemical (such as hydrophobic) surface character nor to differences in atomic surface composition (percentage of nitrogen in particular). As shown elsewhere,[35] water contact angle measurements on APTES-based surfaces as used in this study were consistent with expected values ($53 \pm 2°$) and did not

significantly differ from measurements provided on Br-based NH_2 100% surfaces (55 ± 2°), while contact angle measurements on AHAPS-based NH_2 100% surfaces led to significantly lower values (28 ± 2°). Nitrogen amounts on APTES-, AHAPS-, and Br-based NH_2 100%, as determined by XPS survey spectra, decreased following the APTES- > AHAPS- > Br-based NH_2 100% surfaces ranking (2.7 ± 1.1, 1.7 ± 0.7, and 1.1 ± 0.4%), which is not consistent with variations in bacterial colonization. On the other hand, variations of the extreme surface composition in terms of quantity of functional groups at the molecular scale agreed with bacterial colonization variations. Defects in the structure and organization of APTES- and AHAPS-based NH_2 100% surfaces significantly affect accessibility of NH_2 functional groups at the extreme surface of silane layers as highlighted elsewhere.[35,41] There are fewer NH_2 groups revealed at the extreme surface of AHAPS-based NH_2 100% layers than expected for a fully packed, structured, and organized monolayer (Figure 7d), which is in contrast to what is typically obtained with Br-based NH_2 100% surfaces (Figure 7b). The quantity of NH_2 groups on the extreme surface of APTES-based NH_2 100% surfaces also was less than expected while higher than on AHAPS-based NH_2 100% surfaces (Figure 7c). Trends of variation in NH_2 group accessibility according to NH_2 surface type, thus, agreed with variations between bacterial colonization levels. Insufficient control of APTES- and AHAPS-based NH_2 100% surfaces, in terms of layer structure and organization, also led to high variations in functional group amount at the layer's extreme surface. Consequent low reproducibility between samples of one series probably induced the high variability of results observed in bacterial adhesion tests on APTES- and AHAPS-based NH_2 100% surfaces. Results on AHAPS-based NH_2 100% surfaces were less variable than on APTES-based ones, which is consistent with the higher control of structure and organization observed for AHAPS- in comparison to APTES-based NH_2 100% layers (Figure 7c,d).

This demonstrates that defects in molecular layer may create serious artifacts in microbiological results. Results reliability may be affected through creation of false results or screening of subtle yet relevant other surface-related effects. Besides, variability of defects highly affects the reproducibility of the biological results. Finally, these results point out the relevance of the hereby-developed Br-based surfaces as platforms dedicated to biointerface studies.

4. CONCLUSION

On the basis of the development of an adequate protocol for developing Br−organosilane-based mixed monolayers and a comprehensive surface analysis, we achieved monolayers with a high level of control in terms of chemical composition, silane organization, and layer structure. In particular, Br/CH_3 and NH_2/CH_3 surface fractions were perfectly controlled by the chemical content of the initial Br−organosilane solutions. S_N2 bromine-to-azide and further azide-to-amine chemical conversions that were used to finally obtain NH_2/CH_3 surfaces did not affect the control of the surface fraction, layer structure, and silane organization. Silanes were structured in a densely packed and organized monolayer as expected for SAMs. The relevance of these highly controlled surfaces as platforms for biointerface studies was evaluated by comparing bacterial adhesion on Br-based, NH_2-terminated monolayers to two other NH_2-terminated surface types based on APTES and AHAPS silanes. Variations in adhered bacterial numbers according to NH_2 surface type were consistent with the probable accessibility of NH_2 functional groups at the extreme surface. The quantity of adhered bacteria on Br-based monolayers throughout several experimental replicates was significantly less dispersed than on both of the other SAM types. This indicates that variations in functional group accessibility resulting from defects in or low reproducibility of the fabricated layers can highly affect adhesion or retention of bacteria at the interface. We believe, therefore, that the chemical platforms that were achieved in this work may offer new opportunities due to their high level of control for studying in a comprehensive way microbial and eukaryotic cell behaviors and biological responses at biointerfaces. Through further grafting of biomolecules, these platforms may finally provide promising tools for studying the impact of accessibility of biomolecules immobilized on biomaterials.

■ ASSOCIATED CONTENT

Supporting Information

XPS atomic concentrations for *X* 100% surfaces (*X* = CH_3, Br, N_3, NH_2) and AFM micrographs of 0, 50, and 100% NH_2/CH_3 MMLs, as well as typical XPS high-resolution spectra of silicon wafer substrate and 100% azide-revealing surface. Calculation needed for the estimation of Br/SiOx atomic composition ratio of Br 100% surfaces, as expected to be measured by XPS analysis, is also described. This material is available free of charge via the Internet at http://pubs.acs.org.

■ AUTHOR INFORMATION

Corresponding Author

*Address: Institut de Science des Matériaux de Mulhouse (IS2M, CNRS UMR7361), 15 rue Jean Starcky, BP2488 68057 Mulhouse Cedex, France. E-mail: Lydie.Ploux@uha.fr.

Notes

The authors declare no competing financial interest.

■ ACKNOWLEDGMENTS

We would like to thank Philippe Fioux for performing the XPS measurements as well as Professors Paul Rouxhet and Hamidou Haidara for valuable discussions about this work. We also want to thank the Alsace Region for having provided funding support for this work.

■ REFERENCES

(1) Anselme, K.; Ponche, A.; Ploux, L. In *Comprehensive Biomaterials*; Ducheyne, P., Healy, K., Hutmacher, D., Grainger, D., Kirkpatrick, J., Eds.; Elsevier: Amsterdam, 2011; Vol. 3, pp 235−256.

(2) Boonaert, C. J. P.; Dufrêne, Y. F.; Rouxhet, P. G. In *Encyclopedia Environmental Microbiology*; Bitton, G., Ed.; Wiley: New York, 2002; pp 113−132.

(3) Katsikogianni, M.; Missirlis, Y. F. *Eur. Cells Mater.* **2004**, *8*, 37−57.

(4) Ploux, L.; Ponche, A.; Anselme, K. *J. Adhes. Sci. Technol.* **2010**, *24*, 2165−2201.

(5) Foka, A.; Katsikogianni, M. G.; Anastassiou, E. D.; Spiliopoulou, I.; Missirlis, Y. F. *Eur. Cells Mater.* **2012**, *24*, 386−402.

(6) Gottenbos, B.; Grijpma, D. W.; van der Mei, H. C.; Feijen, J.; Busscher, H. J. *J. Antimicrob. Chemother.* **2001**, *48*, 7−13.

(7) Ploux, L.; Beckendorff, S.; Nardin, M.; Neunlist, S. *Colloids Surf., B* **2007**, *57*, 174−181.

(8) Rzhepishevska, O.; Hakobyan, S.; Ruhal, R.; Gautrot, J.; Barbero, D.; Ramstedt, M. *Biomater. Sci.* **2013**, *1*, 589−602.

(9) Anselme, K.; Bigerelle, M. *Int. Mater. Rev.* **2011**, *56*, 243−266.

(10) Davidson, P. M.; Özçelik, H.; Hasirci, V.; Reiter, G.; Anselme, K. *Adv. Mater.* **2009**, *21*, 3586−3590.
(11) Kargar, M.; Wang, J.; Nain, A. S.; Behkam, B. *Soft Matter* **2012**, *8*, 10254−10259.
(12) Ling, J. F.; Graham, M. V.; Cady, N. C. *Nano LIFE* **2012**, *02*, 1242004.
(13) Ploux, L.; Anselme, K.; Dirani, A.; Ponche, A.; Soppera, O.; Roucoules, V. *Langmuir* **2009**, *25*, 8161−8169.
(14) Fletcher, D. A.; Mullins, R. D. *Nature* **2010**, *463*, 485−492.
(15) Cottenye, N.; Anselme, K.; Ploux, L.; Vebert-Nardin, C. *Adv. Funct. Mater.* **2012**, *22*, 4891−4898.
(16) Margel, S.; Vogler, E. A.; Firment, L.; Watt, T.; Haynie, S.; Sogah, D. Y. *J. Biomed. Mater. Res.* **1993**, *27*, 1463−1476.
(17) Mrksich, M. *Acta Biomater.* **2009**, *5*, 832−841.
(18) Ponche, A.; Ploux, L.; Anselme, K. *J. Adhes. Sci. Technol.* **2010**, *24*, 2141−2164.
(19) Gooding, J. J.; Ciampi, S. *Chem. Soc. Rev.* **2011**, *40*, 2704−2718.
(20) Sullivan, T. P.; Huck, W. T. S. *Eur. J. Org. Chem.* **2003**, *2003*, 17−29.
(21) Aswal, D. K.; Lenfant, S.; Guerin, D.; Yakhmi, J. V.; Vuillaume, D. *Anal. Chim. Acta* **2006**, *568*, 84−108.
(22) Katsikogianni, M.; Missirlis, Y. *J. Mater. Sci.: Mater. Med.* **2010**, *21*, 963−968.
(23) Nilsson, L. M.; Yakovenko, O.; Tchesnokova, V.; Thomas, W. E.; Schembri, M. A.; Vogel, V.; Klemm, P.; Sokurenko, E. V. *Mol. Microbiol.* **2007**, *65*, 1158−1169.
(24) Ostuni, E.; Chapman, R. G.; Liang, M. N.; Meluleni, G.; Pier, G.; Ingber, D. E.; Whitesides, G. M. *Langmuir* **2001**, *17*, 6336−6343.
(25) Haeussling, L.; Ringsdorf, H.; Schmitt, F. J.; Knoll, W. *Langmuir* **1991**, *7*, 1837−1840.
(26) Qian, X.; Metallo, S. J.; Choi, I. S.; Wu, H.; Liang, M. N.; Whitesides, G. M. *Anal. Chem.* **2002**, *74*, 1805−1810.
(27) Wiencek, K. M.; Fletcher, M. *J. Bacteriol.* **1995**, *177*, 1959−1966.
(28) Wiencek, K. M.; Fletcher, M. *Biofouling* **1997**, *11*, 293−311.
(29) Burton, E. A.; Simon, K. A.; Hou, S.; Ren, D.; Luk, Y.-Y. *Langmuir* **2009**, *25*, 1547−1553.
(30) Heise, A.; Menzel, H.; Yim, H.; Foster, M. D.; Wieringa, R. H.; Schouten, A. J.; Erb, V.; Stamm, M. *Langmuir* **1997**, *13*, 723−728.
(31) Heise, A.; Stamm, M.; Rauscher, M.; Duschner, H.; Menzel, H. *Thin Solid Films* **1998**, *327*−*329*, 199−203.
(32) Fryxell, G. E.; Rieke, P. C.; Wood, L. L.; Engelhard, M. H.; Williford, R. E.; Graff, G. L.; Campbell, A. A.; Wiacek, R. J.; Lee, L.; Halverson, A. *Langmuir* **1996**, *12*, 5064−5075.
(33) Balachander, N.; Sukenik, C. N. *Langmuir* **1990**, *6*, 1621−1627.
(34) Shyue, J.-J.; De Guire, M. R.; Nakanishi, T.; Masuda, Y.; Koumoto, K.; Sukenik, C. N. *Langmuir* **2004**, *20*, 8693−8698.
(35) Böhmler, J.; Ploux, L.; Ball, V.; Anselme, K.; Ponche, A. *J. Phys. Chem. C* **2011**, *115*, 11102−11111.
(36) Kwok, D. Y.; Gietzelt, T.; Grundke, K.; Jacobasch, H. J.; Neumann, A. W. *Langmuir* **1997**, *13*, 2880−2894.
(37) Vidal, O.; Longin, R.; Prigent-Combaret, C.; Dorel, C.; Hooreman, M.; Lejeune, P. *J. Bacteriol.* **1998**, *180*, 2442−2449.
(38) Rasband, W. *ImageJ*; U. S. National Institutes of Health: Bethesda, MD, 1997.
(39) Barbot, C.; Bouloussa, O.; Szymczak, W.; Plaschke, M.; Buckau, G.; Durand, J.-P.; Pieri, J.; Kim, J. I.; Goudard, F. *Colloids Surf., A* **2007**, *297*, 221−239.
(40) Brzoska, J. B.; Ben Azouz, I.; Rondelez, F. *Langmuir* **1994**, *10*, 4367−4373.
(41) Caravajal, G. S.; Leyden, D. E.; Quinting, G. R.; Maciel, G. E. *Anal. Chem.* **1988**, *60*, 1776−1786.
(42) Angst, D. L.; Simmons, G. W. *Langmuir* **1991**, *7*, 2236−2242.
(43) Silberzan, P.; Leger, L.; Ausserre, D.; Benattar, J. J. *Langmuir* **1991**, *7*, 1647−1651.
(44) Peter, C.; Vollhardt, K. *Organic Chemistry*; W. H. Freeman: New York, 1987.
(45) Zhang, S.; Koberstein, J. T. *Langmuir* **2012**, *28*, 486−493.
(46) Daugaard, A. E.; Hvilsted, S.; Hansen, T. S.; Larsen, N. B. *Macromolecules* **2008**, *41*, 4321−4327.
(47) Israelachvili, J. N.; Gee, M. L. *Langmuir* **1989**, *5*, 288−289.
(48) Katsikogianni, M. G.; Missirlis, Y. F. *Acta Biomater.* **2010**, *6*, 1107−1118.
(49) Fryxell, G. E.; Mattigod, S. V.; Lin, Y.; Wu, H.; Fiskum, S.; Parker, K.; Zheng, F.; Yantasee, W.; Zemanian, T. S.; Addleman, R. S.; Liu, J.; Kemner, K.; Kelly, S.; Feng, X. *J. Mater. Chem.* **2007**, *17*, 2863−2874.